

UNITE-FND: Reframing Multimodal Fake News Detection through Unimodal Scene Translation

Arka Mukherjee

KIIT Deemed University
Bhubaneswar, India
arka.mukherjee078@gmail.com

Shreya Ghosh

IIT Bhubaneswar
Bhubaneswar, India
shreya@iitbbs.ac.in

Abstract

Multimodal fake news detection typically demands complex architectures and substantial computational resources, posing deployment challenges in real-world settings. We introduce UNITE-FND¹, a novel framework that reframes multimodal fake news detection as a unimodal text classification task. We propose six specialized prompting strategies with Gemini 1.5 Pro, converting visual content into structured textual descriptions, and enabling efficient text-only models to preserve critical visual information. To benchmark our approach, we introduce *Uni-Fakeddit-55k*, a curated dataset family of 55,000 samples each, each processed through our multimodal-to-unimodal translation framework. Experimental results demonstrate that UNITE-FND achieves 92.52% accuracy in binary classification, surpassing prior multimodal models while reducing computational costs by over 10× (TinyBERT variant: 14.5M parameters vs. 250M+ in SOTA models). Additionally, we propose a comprehensive suite of five novel metrics to evaluate image-to-text conversion quality, ensuring optimal information preservation. Our results demonstrate that structured text-based representations can replace direct multimodal processing with minimal loss of accuracy, making UNITE-FND a practical and scalable alternative for resource-constrained environments.

1 Introduction

The rapid proliferation of multimodal fake news (misleading text combined with manipulated images) has emerged as a major threat to information integrity. Social media platforms such as Instagram, Twitter, and Threads accelerate the spread of deceptive content, making automated detection systems critical for mitigating misinformation (Aïmeur et al., 2023). However, existing mul-

timodal fake news detection (FND) methods (Junhao and Xu, 2024; Shen et al., 2024) often require complex architectures and extensive computational resources, posing significant challenges for real-world deployment. For instance, GAMED (Shen et al., 2024) and MAGIC (Junhao and Xu, 2024) require over 250 million parameters, while self-learning models (Chen et al., 2024) scale beyond 7 billion parameters. These resource-intensive approaches create a substantial barrier for researchers and organizations lacking access to large-scale infrastructure. Moreover, the complexity of these systems often necessitates expertise in multiple deep learning frameworks and sophisticated deployment strategies.

We argue the prevailing assumption that multimodal fake news detection must rely on heavy multimodal transformers. Instead, we reframe the problem as a unimodal task by leveraging the vision-language capabilities of large multimodal models (VLMs) such as Gemini 1.5 Pro², GPT-4o³, or Claude 3.5 Sonnet⁴. To the best of our knowledge, this is the first attempt to solve multimodal fake news detection without a dedicated multimodal classifier.

We introduce **UNITE-FND** (**UNI**modal **T**ranslation **E**nhanced **F**ake **N**ews **D**etection), a novel framework that eliminates the need for multimodal deep learning architectures. Instead of directly processing multimodal data, UNITE-FND translates images into structured textual representations using six specialized prompting strategies. This enables the use of lightweight text-only classifiers, preserving critical visual information while dramatically reducing computational overhead. Our framework achieves 92.52% accuracy on 3-way classification using

¹Codebase: <https://anonymous.4open.science/r/UNITE-FND-7118>

Full dataset will be made publicly available upon acceptance.

²<https://blog.google/technology/ai/google-gemini-next-generation-model-february-2024/>

³<https://openai.com/index/hello-gpt-4o/>

⁴<https://www.anthropic.com/news/claude-3-5-sonnet>

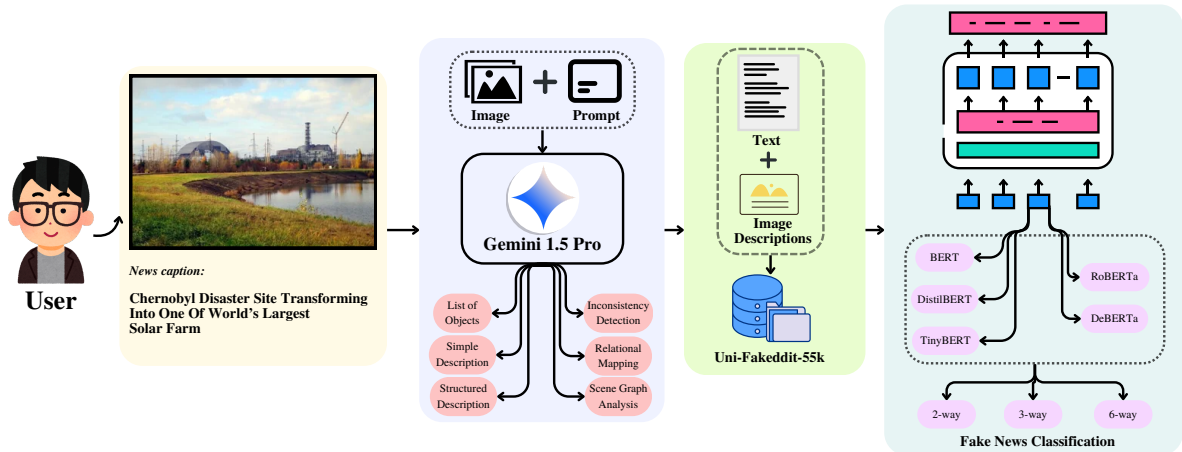


Figure 1: Overview of the UNITE-FND framework. Our approach transforms multimodal fake news detection into a unimodal task through specialized prompting strategies and efficient text classification.

an RTX 4060 laptop GPU, with fine-tuning costs as low as \$1.9, a significant improvement over prior multimodal models requiring cloud-scale resources.

The key contributions of our work include:

1. **UNITE-FND**, a framework that transforms multimodal fake news detection into an efficient unimodal classification task, eliminating the need for heavy multimodal models.
2. We develop **Uni-Fakeddit-55k**, a dataset containing 55,000 samples derived from the Fakeddit (Nakamura et al., 2020) corpus, processed through six structured prompting techniques to maximize visual information extraction.
3. A comprehensive suite of five novel metrics for evaluating image-to-text conversion quality, ensuring effective preservation of critical visual cues.⁵
4. We conduct extensive empirical validation, demonstrating that structured text-based representations can replace multimodal models with minimal accuracy loss, enabling efficient inference on consumer-grade hardware (0.2–8.7GB VRAM).

Our experimental results demonstrate that UNITE-FND achieves comparable or superior performance to existing approaches while dramatically

⁵To support reproducibility and future research, we will publicly release our datasets, prompting templates, and evaluation metrics.

reducing computational overhead. Using DistilBERT, we achieve 88.75% accuracy with only 66M parameters and 0.4GB memory usage, compared to recent approaches requiring 250M+ parameters (Jun-hao and Xu, 2024). This efficiency enables deployment on consumer-grade hardware, making sophisticated fake news detection accessible to a broader range of users and organizations.

2 Related work

2.1 Early Fusion-based Approaches

Early fusion-based approaches established the foundation of multimodal fake news detection, with SpotFake (Singhal et al., 2019) pioneering BERT and VGG-19 integration, while EANN (Wang et al., 2018) introduced event discriminators with VGG and Text-CNN architectures. Basic CNN architectures (Segura-Bedmar and Alonso-Bartolome, 2022) achieved 88% accuracy on Fakeddit, followed by improvements through SpotFake+ (Singhal et al., 2020) (85.6% on GossipCop) and MVAE (Khattar et al., 2019) (82.4% on Weibo). SAFE (Zhou et al., 2020) and CAFE (Jin et al., 2021) advanced fusion mechanisms, while HMCAN (Qian et al., 2021) and VERITE (Papadopoulos et al., 2024) introduced attention-based architectures. These early approaches, while groundbreaking, suffered from rigid fusion mechanisms and limited interaction between modalities.

2.2 Cross-Modal Interaction Frameworks

Sophisticated approaches focusing on modality interactions aim to solve issues with fusion-based techniques. MIMoE-FND (Liu et al., 2025)

achieved 95.6% accuracy on Weibo-21 through mixture-of-experts architecture. MPFN (Wang et al., 2023) introduced progressive fusion networks with 83.8% on Weibo. Recently released CroMe (Choi et al., 2025) achieved 97.4% on Weibo using tri-transformers through better capture of intra-modality relationships. DAAD (Su et al., 2024) and MGCA (Guo et al., 2024) further improved modality interactions through dynamic analysis and multi-granularity alignment. They achieve 94.2% and 91.3% on Weibo-21 respectively.

2.3 Large Model Integration

In recent years, the release of large vision-language models introduced new possibilities, with FND-CLIP (Zhou et al., 2023) achieving 94.2% on PolitiFact. IMFND (Jiang and Wang, 2024) explores GPT4V and CogVLM, though with limited success (80.1% on PolitiFact). A self-learning approach (Chen et al., 2024) leverages LLMs for feature extraction without labeled data, achieving 88.88% on Fakeddit. CMA (Jiang et al., 2025) investigated few-shot learning, though with modest results (79.77% on PolitiFact). These methods primarily use large models as feature extractors or direct classifiers, whereas UNITE-FND innovatively employs Gemini 1.5 Pro as a modality translator, enabling more effective use of specialized text classification models.

2.4 Knowledge-Enhanced Detection

Knowledge-enhanced methods emerged as another direction, with AKA-Fake (Zhang et al., 2024) employing reinforcement learning and GAMED (Shen et al., 2024) introducing multi-expert decoupling (achieving impressive 98.46% results on the specialized Yang dataset). RaCMC (Yu et al., 2024) incorporates multi-granularity constraints with a residual-aware compensation network. These approaches achieve strong performance but require extensive knowledge bases and complex integration mechanisms. Our approach achieves comparable results through Gemini’s inherent knowledge, eliminating the need for external knowledge bases.

2.5 Specialized Approaches

Specialized approaches have also emerged, including AMPLE (Xu et al., 2025) with emotion awareness (90% accuracy on PolitiFact), MMCNFND (Bansal et al., 2024) addressing multilingual challenges across multiple Indic languages (99.6% on

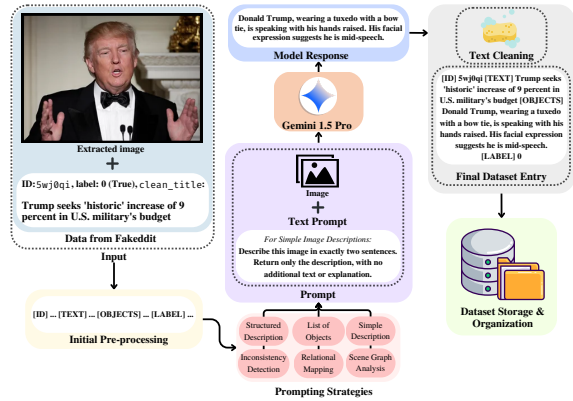


Figure 2: Dataset creation pipeline for Uni-Fakeddit-55k. Each entry from the Fakeddit dataset is processed using six specialized prompting strategies with Gemini 1.5 Pro for image-to-text conversion. The pipeline consists of initial preprocessing, parallel prompting pathways, and structured dataset organization, generating six complementary text-based representations.

MMIFND), and MAGIC framework (Jun-hao and Xu, 2024) using geometric deep learning (98.8% accuracy on a curated subset of Fakeddit with 3,127 samples). While these methods excel in specific scenarios, UNITE-FND provides a more generalizable solution through its modality translation.

3 UNITE-FND

UNITE-FND redefines multimodal fake news detection by transforming complex multimodal analysis into a streamlined unimodal task. The key innovation lies in leveraging state-of-the-art Large Language Models (LLMs) to convert visual content into structured textual descriptions, enabling efficient text-only classification without sacrificing critical visual information.

3.1 Image-to-Text Conversion Framework

At the core of our approach is a robust image-to-text conversion framework powered by Gemini 1.5 Pro, a state-of-the-art multimodal large language model (LLM). We design a structured prompting strategy consisting of six distinct methods, each tailored to extract different aspects of visual information.

3.1.1 Basic Object Identification

The first method employs a List of Objects approach, utilizing a carefully crafted prompt to generate a comprehensive CSV-formatted inventory of distinct objects within the image. This

method ensures the capture of fundamental visual elements while maintaining a structured, machine-processable output format. Figure 4 illustrates our proposed pipeline⁶.

3.1.2 Contextual Description Generation

To enhance semantic richness, we incorporate two complementary descriptive approaches: Simple Image Description and Structured Image Description. Both methods generate dual-sentence descriptions, with the first sentence capturing observable facts and the second providing contextual interpretation. This dual-layer approach ensures both concrete visual information and implied contextual cues are preserved (Refer Appendix F for examples).

3.1.3 Spatial Analysis

The Relational Mapping framework systematically catalogs spatial relationships through a structured JSON schema. Each object is assigned a unique identifier and location descriptor, while relationships between objects are documented with specific interaction types and confidence scores. This approach transforms complex visual-spatial information into a machine-readable format, capturing both direct physical relationships (like "above" or "next to") and interactive associations (such as "facing" or "holding"). The framework prioritizes high-confidence relationships, ensuring reliability in downstream processing while maintaining a clear representation of the image’s spatial hierarchy. This method proves particularly valuable for fact-checking claims about spatial arrangements in news photos, such as verifying the authenticity of crowd sizes or the relative positioning of people in event coverage.

3.1.4 Manipulation Detection Components

Two specialized components focus on identifying potential image manipulations:

- **Inconsistency Detection:** Performs a comprehensive analysis of visual coherence, examining lighting, perspective, boundaries, and resolution patterns. This component generates structured JSON output detailing potential manipulation indicators with associated confidence scores.
- **Scene Graph Analysis:** Creates a detailed representation of the image scene, capturing

⁶Due to page limitations, examples for each strategy are provided in Appendix F

object relationships, visual quality metrics, and potential manipulation artifacts. This component provides a holistic view of the image’s structural integrity.

These components are especially effective for scenarios requiring detailed forensic analysis, such as investigating claims of digital tampering in politically sensitive images or verifying the authenticity of emergency situation photographs.

3.2 Uni-Fakeddit-55k Dataset Creation and Classification Pipeline

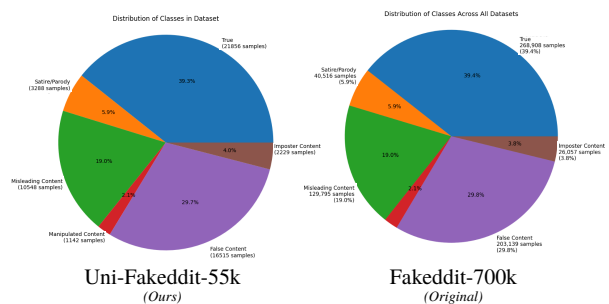


Figure 3: Distribution comparison between our Uni-Fakeddit-55k dataset (left) and the original Fakeddit-700k dataset (right). The pie charts demonstrate that our sampling strategy preserves the relative proportions of different content categories while creating a more manageable dataset size. Both datasets maintain similar class distributions across six categories: True, Satire/Parody, Misleading Content, Manipulated Content, False Content, and Imposter Content, with variations of less than 0.5% in relative proportions.

Our work introduces a family of six unimodal datasets, collectively called Uni-Fakeddit-55k, derived from the multimodal Fakeddit-700k dataset. Each dataset variant corresponds to one of our six prompting techniques, offering different perspectives on the same underlying content. Figure 3 illustrates the careful sampling strategy employed to maintain class distribution consistency with the original dataset. More details about the exact prompts and settings used to build the datasets are reported in Appendix F.

The textual descriptions generated by our six-component framework undergo several processing steps:

$$T_{final} = f_{merge}(T_{clean}, T_{desc}) \quad (1)$$

where T_{clean} represents the cleaned news title, T_{desc} represents the concatenated image descrip-

tions, and f_{merge} is our custom text merger function.

The processed text is then passed through a selection of text-only models: BERT, DistilBERT, TinyBERT, RoBERTa-Large, and DeBERTa-V3-Large.

Each model is fine-tuned on our processed dataset using the following objective:

$$\mathcal{L} = - \sum_{i=1}^N y_i \log(\hat{y}_i) + \lambda \|\theta\|_2 \quad (2)$$

where y_i represents the true label, \hat{y}_i is the model prediction, and λ controls the L2 regularization strength.

Using this pipeline, we effectively transform the complex task of multimodal fake news detection into a more tractable text-only classification problem while preserving critical visual information through our sophisticated image-to-text conversion framework.



Figure 4: Illustration of the List of Objects prompting approach. The system takes two inputs: (1) a carefully engineered text prompt that requests a comma-separated list of distinct, identifiable objects, and (2) the target image (shown: futuristic cityscape with Eiffel Tower). Gemini 1.5 Pro processes these inputs to generate a structured CSV output containing all major visible objects.

3.3 UNITE-FND Model Architecture: Optimized for Resource-Constrained Environments

While recent approaches have achieved impressive accuracy through increasingly complex architectures, UNITE-FND prioritizes efficiency without significant performance trade-offs. As shown in Table 5, current state-of-the-art approaches like MAGIC (Jun-hao and Xu, 2024) and GAMED (Shen et al., 2024) require over 250 million parameters, while self-learning approaches exceed 7 billion parameters. In contrast, our most efficient implementation using TinyBERT requires only 14.5 million parameters while achieving 87.4% accuracy on Uni-Fakeddit-55k. Even our

largest model variant using DeBERTa-large (400M parameters) requires significantly fewer parameters than certain contemporary approaches while achieving a competitive accuracy of 92.5%.

This efficiency translates directly into practical advantages: (a) Our models require as little as 0.2GB VRAM (TinyBERT) and scale up to just 8.7GB (DeBERTa), enabling deployment on consumer-grade hardware without the need for specialized infrastructure. (b) The cost-effectiveness of our approach is equally notable, with full model fine-tuning achievable for as little as \$2 using cloud-based compute resources. (c) Additionally, the flexibility of UNITE-FND allows organizations to select model variants that best align with their accuracy-efficiency trade-offs, making it adaptable to diverse operational constraints. These characteristics position UNITE-FND as a highly scalable solution for resource-constrained environments while maintaining performance competitive with significantly more complex architectures.

4 Evaluation Metrics

To comprehensively evaluate the quality and effectiveness of our image-to-text conversion framework, we propose a novel suite of five complementary metrics, each designed to capture different aspects of information preservation and transfer quality. These metrics are then combined into a unified Composite Information Quality Score (CIQS).

4.1 Image Preservation Rate (IPR)

The Image Preservation Rate quantifies how effectively the textual description retains the essential information present in the original image. We improve upon traditional correlation-based approaches by introducing a non-linear transformation that better captures the relationship between feature spaces. Let I be the image features and T be the text embeddings:

$$IPR(I, T) = 1 - e^{-5s} \quad (3)$$

where s represents the scaled cosine similarity between normalized projections P_I and P_T in a common space of dimension $d = \min(\dim(I), \dim(T))$:

$$s = \frac{\cos(P_I, P_T) + 1}{2} \quad (4)$$

The projections are obtained through Xavier-initialized linear transformations to ensure stable feature mapping across modalities.

4.2 Semantic Coverage Score (SCS)

SCS evaluates the comprehensiveness of the generated description, focusing on object-centric content. For object list techniques, we employ a multi-criteria evaluation:

$$SCS(T) = w_l \cdot L + w_s \cdot S + w_c \cdot C \quad (5)$$

where $L = \min(|O|/10, 1.0)$ represents the normalized object count, S quantifies specificity by penalizing generic terms, and C measures completeness based on the presence of multi-word descriptions. The weighting factors are set as $w_l = 0.3$, $w_s = 0.4$, and $w_c = 0.3$.

4.3 Information Specificity Score (ISS)

ISS measures the semantic depth and specificity of the generated description:

$$ISS(T) = \frac{1}{|W|} \sum_{w \in W} \frac{D(w)}{D_{max}} \quad (6)$$

where W is the set of content words, $D(w)$ represents the WordNet depth of word w , and D_{max} is the maximum WordNet depth (approximately 20).

4.4 Structural Information Retention (SIR)

SIR evaluates the preservation of structural relationships, with distinct formulations for different technique types:

(1) For graph-based techniques:

$$SIR(G) = \frac{1}{4}(N_s + E_d + R_d + C_s) \quad (7)$$

where: $N_s = \min(|V|/10, 1)$ represents the node score, E_d is the edge density, $R_d = \min(|R|/5, 1)$ measures relationship diversity and $C_s = \frac{conf_V + conf_E}{2}$ indicates confidence score.

(2) For text-based techniques:

$$SIR(T) = \frac{|S|}{5} \quad (8)$$

where S is the set of sentences.

4.5 Modality Transfer Efficiency (MTE)

MTE assesses both the efficiency of information transfer and preservation of feature complexity:

$$MTE(I, T) = 0.7 \cdot S + 0.3 \cdot C_r \quad (9)$$

where S represents cosine similarity between normalized projections, $C_r = \frac{\min(\sigma_I, \sigma_T)}{\max(\sigma_I, \sigma_T)}$ measures complexity ratio, σ_I, σ_T are standard deviations of projected features.

4.6 Composite Information Quality Score (CIQS)

Finally, we combine all metrics into a single comprehensive score:

$$CIQS = (IPR \cdot SCS \cdot ISS \cdot SIR \cdot MTE)^{\frac{1}{5}} \quad (10)$$

This geometric mean ensures a balanced contribution from all components while penalizing poor performance in any single metric. The CIQS provides a holistic assessment of the image-to-text conversion quality, considering preservation, coverage, specificity, structure, and transfer efficiency.

5 Results

5.1 Quality of Image-to-Text Conversion

We first evaluate the quality of our image-to-text conversion strategies using our proposed metrics suite (Table 1), where each metric is normalized to a [0,1] range except for SIR which can exceed 1 due to its structural complexity measure. All strategies demonstrate strong Information Preservation Rate ($IPR > 0.91$), indicating effective retention of core visual information. Scene Graph Analysis and Inconsistency Detection achieve particularly high Semantic Coverage Scores ($SCS > 0.96$), suggesting comprehensive capture of image content. While List of Objects shows the highest Information Specificity Score ($ISS = 0.4635$), Scene Graph Analysis excels in Structural Information Retention ($SIR = 2.1231$), reflecting its superior ability to preserve relational information. Modality Transfer Efficiency (MTE) remains consistent across all strategies (0.65), indicating stable information transfer between modalities.

5.2 Classification Performance

5.2.1 Comparison with Vision-Language Models

UNITE-FND framework achieves state-of-the-art performance on the Uni-Fakeddit-55k dataset, significantly outperforming existing vision-language models (Table 2). The framework achieves 92.52% accuracy in binary classification, substantially surpassing recent models like Llama-3.2-11B-Vision (63.92%) and Video-LLaVA-7B (59.34%). This marked improvement demonstrates the effectiveness of our modality translation approach over direct multimodal processing.

Prompting Strategy	IPR	SCS	ISS	SIR	MTE	CIQS
List of Objects	0.9176	0.7417	0.4635	0.2030	0.6498	0.5268
Simple Image Description	0.9176	0.7690	0.3925	0.4049	0.6497	0.5910
Structured Image Description	0.9175	0.8148	0.3727	0.3805	0.6498	0.5827
Relational Mapping	0.9176	0.9243	0.4102	0.2055	0.6497	0.5396
Inconsistency Detection	0.9175	0.9780	0.2802	0.9443	0.6497	0.6742
Scene Graph Analysis	0.9176	0.9668	0.3677	2.1231	0.6497	0.8484

Table 1: Evaluation Metrics Across Different Prompting Strategies on Uni-Fakeddit-55k

Model	Accuracy (%)
LanguageBind/ Video-LLaVA-7B-hf	59.34
Salesforce/ instructblip-vicuna-7b meta-llama/ Llama-3.2-11B-Vision	59.35
UNITE-FND (Ours)	92.52

Table 2: Binary Classification Accuracy on Uni-Fakeddit-55k Dataset

5.2.2 Comparison with Existing Fake News Detection Model

When compared to existing multimodal fake news detection systems (Table 3), UNITE-FND demonstrates substantial improvements across all metrics. Our framework achieves gains of:

- **Accuracy:** +3.64% (\uparrow over Self-learning (Chen et al., 2024))
- **Precision:** +6.16% (\uparrow over SpotFake+ (Singhal et al., 2020))
- **Recall:** +7.23% (\uparrow over CAFE (Jin et al., 2021))
- **F1-score:** +6.63% (\uparrow over Self-learning (Chen et al., 2024))

These results demonstrate that our approach of converting multimodal fake news detection into a unimodal problem through sophisticated image-to-text conversion not only simplifies the architecture but also leads to superior performance. The consistent improvements across all metrics suggest that our framework better captures the nuanced relationships between visual and textual content in fake news detection.

While our results demonstrate strong performance, it is essential to consider variations in

Model	Acc	P	R	F1
MVAE (Khattar et al., 2019)	70.24	76.53	74.75	75.63
EANN (Wang et al., 2018)	72.27	78.43	63.40	70.12
SpotFake (Singhal et al., 2019)	77.29	71.63	70.77	71.20
HMCAN (Qian et al., 2021)	82.89	84.03	84.04	84.03
SpotFake+ (Singhal et al., 2020)	83.08	86.38	84.87	85.62
CAFE (Jin et al., 2021)	84.14	85.39	85.27	85.32
VERITE (Papadopoulos et al., 2024)	84.72	85.34	84.37	84.85
Self-learning (Chen et al., 2024)	88.88	86.40	85.40	85.90
UNITE-FND (Ours)	92.52	92.56	92.50	92.53

Note: All metrics are percentages. Experiments conducted on a 10% subset of the Fakeddit dataset for fair comparison.

Table 3: Performance Comparison of Fake News Detection Models on Fakeddit (10% subset)

evaluation metrics when comparing across different dataset splits. Prior work (Shen et al., 2024) shows that models such as EANN and MVAE achieve substantially higher accuracy on the full Fakeddit dataset (87.5% and 88.75%, respectively) compared to their performance on a 10% subset (72.27% and 70.24%). More recent advancements further push performance boundaries, with GAMED reaching 93.93%, followed by CLIP+LLaVA at 92.54% and BMR at 91.65%. These trends suggest that model performance bene-

fits significantly from larger training sets. Although direct comparisons across different dataset configurations must be interpreted cautiously, it is important to note that UNITE-FND achieves 92.52% accuracy using only a 10% subset of Fakeddit. Despite being trained on significantly less data, our approach remains highly competitive with state-of-the-art multimodal models evaluated on the full dataset. This underscores the effectiveness of structured image-to-text conversion in preserving critical visual information while reducing computational complexity.

5.3 Observations on Proposed Evaluation Metrics

Analysis of our evaluation metrics (Table 1) reveals distinct patterns that offer key insights into the effectiveness of different prompting strategies. All techniques exhibit consistently high Information Preservation Rates (IPR \approx 0.917), which explains the substantial improvements observed over text-only baselines.

Observation 1. The Semantic Coverage Score (SCS) highlights a clear distinction between simpler and more sophisticated approaches. JSON-based methods such as Scene Graph (0.9668) and Inconsistency Detection (0.9780) achieve significantly higher coverage than simpler strategies like List of Objects (0.7417). However, this increased coverage does not translate into proportional classification gains, suggesting that transformer models may not fully exploit the additional structured information.

Observation 2. A notable inverse relationship emerges between technique sophistication and Information Specificity Scores (ISS). Simpler methods, such as List of Objects (0.4635), outperform more complex strategies like Scene Graph (0.3677). This pattern suggests that while structured representations capture extensive visual information, they may introduce noise that hinders model interpretability.

Observation 3. The Structural Information Retention (SIR) metric shows considerable variation, with Scene Graph Analysis achieving the highest score (2.1231) due to its detailed encoding of spatial relationships. Interestingly, Relational Mapping performs worse (0.2055) than even basic descriptions, likely because it emphasizes object interactions rather than spatial structure.

Observation 4. The Composite Information Quality Score (CIQS) presents an unexpected discrep-

ancy: Scene Graph Analysis achieves the highest CIQS (0.8484) but ranks second in classification performance, whereas Structured Image Description, which ranks fourth in CIQS (0.5827), consistently outperforms other techniques across transformer architectures. This suggests that *maximizing information capture alone is insufficient*; rather, effective fake news detection requires balancing information complexity with model interpretability and processing efficiency.

These findings highlight the importance of our proposed evaluation metrics that not only capture rich multimodal information but also align with model interpretability and processing capabilities. By providing deeper insights into the relationship between structured textual representations and classification performance, our metrics offer a valuable framework for optimizing multimodal-to-unimodal transformations in misinformation detection.

6 Conclusion and Future Works

We present UNITE-FND, a novel framework that reframes multimodal fake news detection as a unimodal task through structured image-to-text conversion. Our approach significantly reduces computational overhead while maintaining competitive accuracy, enabling deployment on consumer-grade hardware. Experimental results demonstrate that structured textual representations effectively replace direct multimodal processing with minimal performance loss, highlighting the potential of language models in preserving critical visual information. Future work can explore adaptive prompt optimization, multilingual adaptation, and temporal modeling to enhance robustness. Additionally, improving explainability and mitigating adversarial vulnerabilities will be crucial for responsible deployment. By balancing efficiency, accessibility, and interpretability, UNITE-FND lays the foundation for scalable, real-world misinformation detection.

Limitations

While UNITE-FND shows promising results, there are few limitations. First, our approach’s reliance on VLMs (specifically Gemini 1.5 Pro) for image-to-text conversion introduces a potential bottleneck in processing speed. Second, the quality of text generation can vary based on the VLM’s understanding of complex visual scenarios. Third, while our method significantly reduces computational requirements for deployment, it still requires access

to the Gemini API, which may present cost considerations for large-scale applications.

Ethical Considerations

Our work utilizes the Fakeddit dataset, which contains Reddit posts that have been carefully curated and pre-processed by its creators to address privacy and ethical concerns. Given the dataset’s thorough preparation, which includes removal of personally identifiable information and offensive content, we maintained its existing privacy safeguards without additional processing to preserve data integrity and statistical properties. Our image-to-text conversion strategies are designed to extract only objective visual elements, ensuring that generated descriptions exclude references to specific individuals or private information. While our approach enhances accessibility and efficiency in fake news detection, we recognize the potential risks associated with its misuse, including the possibility of censorship or content manipulation. We advocate for responsible and transparent use, respecting individual privacy and freedom of expression, with clear communication about its deployment and the option for users to opt-out. We acknowledge the possibility for potential false positives and false negatives, and we suggest continuous research, development, and stakeholder feedback for system refinement. We declare no competing interests. The research was conducted independently, and the framework was developed for academic and public benefit aiming to better understand and fight misinformation online.

References

- Esma Aïmeur, Soumaya Amri, and Gilles Brassard. 2023. [Fake news, disinformation and misinformation in social media: a review](#). *Social Network Analysis and Mining*, 13(30).
- Shubhi Bansal, Nishit Sushil Singh, Shahid Shafi Dar, and Nagendra Kumar. 2024. [Mmcfnd: Multimodal multilingual caption-aware fake news detection for low-resource indic languages](#). *Preprint*, arXiv:2410.10407.
- Hao Chen, Hui Guo, Baochen Hu, Shu Hu, Jinrong Hu, Siwei Lyu, Xi Wu, and Xin Wang. 2024. [A self-learning multimodal approach for fake news detection](#). *Preprint*, arXiv:2412.05843.
- Eunjee Choi, Junhyun Ahn, XinYu Piao, and Jong-Kook Kim. 2025. [Crome: Multimodal fake news detection using cross-modal tri-transformer and metric learning](#). *Preprint*, arXiv:2501.12422.
- Hao Guo, Zihan Ma, Zhi Zeng, Minnan Luo, Weixin Zeng, Jiuyang Tang, and Xiang Zhao. 2024. [Each fake news is fake in its own way: An attribution multi-granularity benchmark for multimodal fake news detection](#). *Preprint*, arXiv:2412.14686.
- Ye Jiang, Taihang Wang, Xiaoman Xu, Yimin Wang, Xingyi Song, and Diana Maynard. 2025. [Cross-modal augmentation for few-shot multimodal fake news detection](#). *Engineering Applications of Artificial Intelligence*, 142:109931.
- Ye Jiang and Yimin Wang. 2024. [Large visual-language models are also good classifiers: A study of in-context multimodal fake news detection](#). *Preprint*, arXiv:2407.12879.
- Xiao Jin, Pin-Yu Chen, Chia-Yi Hsu, Chia-Mu Yu, and Tianyi Chen. 2021. [Cafe: catastrophic data leakage in vertical federated learning](#). In *Proceedings of the 35th International Conference on Neural Information Processing Systems, NIPS ’21*, Red Hook, NY, USA. Curran Associates Inc.
- Jun-hao and Xu. 2024. [A multimodal adaptive graph-based intelligent classification model for fake news](#). *Preprint*, arXiv:2411.06097.
- Dhruv Khattar, Jaipal Singh Goud, Manish Gupta, and Vasudeva Varma. 2019. [Mvae: Multimodal variational autoencoder for fake news detection](#). In *The World Wide Web Conference, WWW ’19*, page 2915–2921, New York, NY, USA. Association for Computing Machinery.
- Yifan Liu, Yaokun Liu, Zelin Li, Ruichen Yao, Yang Zhang, and Dong Wang. 2025. [Modality interactive mixture-of-experts for fake news detection](#). *Preprint*, arXiv:2501.12431.
- Kai Nakamura, Sharon Levy, and William Yang Wang. 2020. [Fakeddit: A new multimodal benchmark dataset for fine-grained fake news detection](#). In *Proceedings of the Twelfth Language Resources and Evaluation Conference*, pages 6149–6157, Marseille, France. European Language Resources Association.
- Stefanos-Iordanis Papadopoulos, Christos Koutlis, Symeon Papadopoulos, and Panagiotis C. Petrantonakis. 2024. [Verite: a robust benchmark for multimodal misinformation detection accounting for unimodal bias](#). *International Journal of Multimedia Information Retrieval*, 13(1):4.
- Shengsheng Qian, Jinguang Wang, Jun Hu, Quan Fang, and Changsheng Xu. 2021. [Hierarchical multi-modal contextual attention network for fake news detection](#). In *Proceedings of the 44th International ACM SIGIR Conference on Research and Development in Information Retrieval, SIGIR ’21*, page 153–162, New York, NY, USA. Association for Computing Machinery.
- Isabel Segura-Bedmar and Santiago Alonso-Bartolome. 2022. [Multimodal fake news detection](#). *Information*, 13(6).

- Lingzhi Shen, Yunfei Long, Xiaohao Cai, Imran Razzak, Guanming Chen, Kang Liu, and Shoaib Jameel. 2024. [Gamed: Knowledge adaptive multi-experts decoupling for multimodal fake news detection](#). *Preprint*, arXiv:2412.12164.
- Shivangi Singhal, Anubha Kabra, Mohit Sharma, Rajiv Ratn Shah, Tanmoy Chakraborty, and Ponnurangam Kumaraguru. 2020. [Spotfake+: A multi-modal framework for fake news detection via transfer learning \(student abstract\)](#). *Proceedings of the AAAI Conference on Artificial Intelligence*, 34(10):13915–13916.
- Shivangi Singhal, Rajiv Ratn Shah, Tanmoy Chakraborty, Ponnurangam Kumaraguru, and Shin'ichi Satoh. 2019. [Spotfake: A multi-modal framework for fake news detection](#). In *2019 IEEE Fifth International Conference on Multimedia Big Data (BigMM)*, pages 39–47.
- Xinqi Su, Yawen Cui, Ajian Liu, Xun Lin, Yuhao Wang, Haochen Liang, Wenhui Li, and Zitong Yu. 2024. [Daad: Dynamic analysis and adaptive discriminator for fake news detection](#). *Preprint*, arXiv:2408.10883.
- Yaqing Wang, Fenglong Ma, Zhiwei Jin, Ye Yuan, Guangxu Xun, Kishlay Jha, Lu Su, and Jing Gao. 2018. [Eann: Event adversarial neural networks for multi-modal fake news detection](#). In *Proceedings of the 24th ACM SIGKDD International Conference on Knowledge Discovery & Data Mining, KDD '18*, page 849–857, New York, NY, USA. Association for Computing Machinery.
- Yuxiang Wang, Ming Yang, Xingyu Chen, and Peng Wang. 2023. Multimodal fake news detection via progressive fusion networks. *Information Processing & Management*.
- Xiaoman Xu, Xiangrun Li, Taihang Wang, and Ye Jiang. 2025. [Ample: Emotion-aware multimodal fusion prompt learning for fake news detection](#). In *Multimedia Modeling*, pages 86–100, Singapore. Springer Nature Singapore.
- Xinquan Yu, Ziqi Sheng, Wei Lu, Xiangyang Luo, and Jiantao Zhou. 2024. [Racmc: Residual-aware compensation network with multi-granularity constraints for fake news detection](#). *Preprint*, arXiv:2412.18254.
- Litian Zhang, Xiaoming Zhang, Ziyi Zhou, Feiran Huang, and Chaozhuo Li. 2024. [Reinforced adaptive knowledge learning for multimodal fake news detection](#). *Proceedings of the AAAI Conference on Artificial Intelligence*, 38(15):16777–16785.
- Xinyi Zhou, Jindi Wu, and Reza Zafarani. 2020. [Safe: Similarity-aware multi-modal fake news detection](#). In *Advances in Knowledge Discovery and Data Mining*, pages 354–367, Cham. Springer International Publishing.
- Yangming Zhou, Yuzhou Yang, Qichao Ying, Zhenxing Qian, and Xinpeng Zhang. 2023. [Multimodal fake news detection via clip-guided learning](#). In *2023 IEEE International Conference on Multimedia and Expo (ICME)*, pages 2825–2830.

Appendices

This supplementary material presents additional details on the following aspects:

- **Appendix A:** Literature Review (in details)
- **Appendix B:** Model Architecture and Performance Studies
- **Appendix C:** Ablation Studies
- **Appendix D:** Training Costs
- **Appendix E:** Gemini 1.5 Pro - Why?
- **Appendix F:** Prompting Techniques and Examples
- **Appendix G:** Training Hyperparameters
- **Appendix H:** Vision-Language Model Testing Configuration

A Literature Review

This appendix provides a comprehensive review of multimodal fake news detection approaches, organized by their methodological focus and chronological development.

A.1 Early Fusion-based Approaches (2019-2022)

Early work in multimodal fake news detection established foundational architectures for combining visual and textual information:

- SpotFake (Singhal et al., 2019) pioneered multimodal fusion using BERT and VGG-19, achieving 89.23% accuracy on Weibo
- MVAE (Khattar et al., 2019) introduced a bimodal variational autoencoder approach, reaching 82.4% accuracy on Weibo
- SpotFake+ (Singhal et al., 2020) enhanced the architecture with XLNet, achieving 85.6% on GossipCop
- SAFE (Zhou et al., 2020) introduced similarity-aware fusion, reaching 87.4
- MM-CNN (Segura-Bedmar and Alonso-Bartolome, 2022) demonstrated that basic CNN architectures could achieve 87.0% accuracy on Fakeddit

A.2 Advanced Architectures (2023-2024)

Recent approaches have introduced more sophisticated architectural innovations:

- MPFN (Wang et al., 2023) explored progressive fusion to capture both shallow and deep features (83.8% on Weibo)
- FND-CLIP (Zhou et al., 2023) leveraged CLIP’s pre-trained representations (94.2% on PolitiFact)
- MAGIC (Jun-hao and Xu, 2024) introduced graph neural networks, achieving 98.8% on a curated Fakeddit subset
- GAMED (Shen et al., 2024) employed modal decoupling with expert networks (93.93% on Fakeddit)
- RaCMC (Yu et al., 2024) introduced residual-aware compensation networks (92.2% on Weibo-21)

A.3 Knowledge-Enhanced Methods

Several approaches have incorporated external knowledge:

- AKA-Fake (Zhang et al., 2024) used reinforcement learning for knowledge graph construction (91.9% on PolitiFact)
- AMPLE (Xu et al., 2025) integrated emotion-aware analysis (90% on PolitiFact)
- DAAD (Su et al., 2024) introduced dynamic analysis mechanisms (94.2% on Weibo-21)

A.4 Large Model Integration

Recent work has explored the potential of large vision-language models:

- IMFND (Jiang and Wang, 2024) investigated zero-shot capabilities of GPT4V (80.1% on PolitiFact)
- CroMe (Choi et al., 2025) combined BLIP2 with tri-transformers (97.4% on Weibo)
- MIMoE-FND (Liu et al., 2025) introduced mixture-of-experts architecture (95.6% on Weibo-21)

A.5 Specialized Applications

Several approaches have focused on specific challenges:

- MCMFND (Bansal et al., 2024) addressed multilingual detection, achieving 99.6% on MMIFND
- Self-Learning FND (Chen et al., 2024) explored unlabeled data utilization (88.88% on Fakeddit)
- MGCA (Guo et al., 2024) introduced multi-granularity clue alignment (91.3% on Weibo-21)

Method	Key Components	Best Performance (Dataset)
SpotFake+ (Singhal et al., 2020)	BERT + VGG-19	85.6% (GossipCop)
SAFE (Zhou et al., 2020)	Similarity-aware fusion	87.4% (PolitiFact)
MM-CNN (Segura-Bedmar and Alonso-Bartolome, 2022)	Multimodal CNNs	87.0% (Fakeddit)
MPFN (Wang et al., 2023)	Progressive fusion	83.8% (Weibo)
FND-CLIP (Zhou et al., 2023)	CLIP + feature concat	94.2% (PolitiFact)
MAGIC (Jun-hao and Xu, 2024)	Graph Neural Networks	98.8% (Fakeddit)*
IMFND (Jiang and Wang, 2024)	GPT4V + Zero-shot	80.1% (PolitiFact)
MMCFND (Bansal et al., 2024)	Multilingual encoders	99.6% (MMIFND)
GAMED (Shen et al., 2024)	Modal decoupling + Expert networks	93.93% (Fakeddit)
AKA-Fake (Zhang et al., 2024)	Knowledge graphs + RL	91.9% (PolitiFact)
CroMe (Choi et al., 2025)	Tri-Transformer + BLIP2	97.4% (Weibo)
MIMoE-FND (Liu et al., 2025)	Mixture-of-Experts	95.6% (Weibo-21)
UNITE-FND (Ours)	Multi-strategy Vision Translation + DeBERTa	92.52% (Fakeddit)

*Using a carefully curated set of just 3,127 samples from Fakeddit

Table 4: Comparison of Recent Multimodal Fake News Detection Approaches

A.6 Dataset Usage Patterns

Analysis of the literature reveals several commonly used datasets:

- Weibo and Weibo-21: Popular for Chinese content evaluation
- PolitiFact and GossipCop: Standard benchmarks for English news
- Fakeddit: Largest dataset, often used for a comprehensive evaluation
- Specialized datasets: MMIFND (multilingual), Yang (domain-specific)

This comprehensive review demonstrates the field’s evolution from simple fusion approaches to sophisticated architectures incorporating large models and specialized techniques. Our UNITE-FND framework builds upon these advances while introducing a novel approach to modality translation that achieves competitive performance with reduced computational requirements.

B Model Architecture and Performance Studies

While the main paper focuses on UNITE-FND’s key contributions and primary results, this appendix provides a detailed comparison of model architectures and their respective performance metrics. Table 5 presents a comprehensive overview of recent approaches in multimodal fake news detection,

highlighting the relationship between model complexity and detection accuracy.

Current state-of-the-art approaches demonstrate a clear trend toward increasingly complex architectures. MAGIC (Jun-hao and Xu, 2024) and GAMED (Shen et al., 2024) employ sophisticated neural networks with over 250 million parameters each, while self-learning approaches (Chen et al., 2024) utilize large language models ranging from 7.2 to 13.2 billion parameters. These approaches achieve impressive accuracy but at substantial computational cost.

UNITE-FND, in contrast, demonstrates that efficient architectures can achieve competitive performance through effective modality translation. Our implementation spans a range of model sizes:

- TinyBERT (14.5M parameters) achieves 87.4% accuracy, matching the performance of more complex multimodal architectures while using fewer parameters than even basic unimodal CNNs from earlier approaches (Segura-Bedmar and Alonso-Bartolome, 2022)
- DistilBERT (66M parameters) and BERT-base (110M parameters) demonstrate that moderate-sized models can achieve strong performance (88.8% and 89.2% respectively)
- Our larger models, RoBERTa-large (355M parameters) and DeBERTa-large (400M parameters), achieve competitive accuracy (91.5% and 92.5%) while still maintaining signifi-

Paper	Model	Parameters	Dataset	Accuracy	
Multimodal FND (Segura-Bedmar and Alonso-Bartolome, 2022)	Unimodal CNN	15.2M	Fakeddit	74.0%	
	Unimodal BiLSTM	15.3M		75.0%	
	Unimodal BERT	110M		76.0%	
	Multimodal CNN	22.4M		88.0%	
GAMED (Shen et al., 2024)	GAMED	258M	Fakeddit	93.9%	
			Yang	98.5%	
MAGIC (Jun-hao and Xu, 2024)	MAGIC	252M	Fakeddit	98.8%	
			MChinese	86.3%	
Self-Learning FND (Chen et al., 2024)	N/A	7.2B-13.2B	Fakeddit	88.9%	
UNITE-FND (Ours)	TinyBERT	14.5M	Uni-Fakeddit	87.4%	
	DistilBERT	66M		88.8%	
	BERT-base	110M		-55k	89.2%
	RoBERTa-large	355M		91.5%	
	DeBERTa-large	400M		92.5%	

Note: Parameter counts are rounded to the nearest million (M) or billion (B). Accuracy reported for Fakeddit is on 2-way classification unless otherwise specified.

Table 5: Comparison of Model Architectures and Performance Metrics

cantly lower parameter counts than contemporary approaches

This analysis supports our main paper’s argument that effective modality translation can enable simpler, more efficient architectures to achieve competitive performance in fake news detection. The consistent performance across model sizes suggests that our approach’s effectiveness stems from the quality of the image-to-text conversion rather than raw model capacity.

C Ablation Studies

Detailed analysis of model performance across different architectures (Table 6) reveals several significant patterns and insights. RoBERTa-large demonstrates superior performance across all classification settings, particularly with the Structured Image Description technique, achieving 87.95%, 91.45%, and 91.88% accuracy on 6-way, 3-way, and 2-way classification tasks respectively. This represents substantial improvements over its text-only baseline (78.80%, 86.99%, 87.23%).

The performance scaling across model sizes is particularly noteworthy. TinyBERT, despite its compact architecture, shows remarkable improvements with visual information integration, achieving up to 87.36% accuracy in binary classification

compared to its 83.24% text-only baseline. DistilBERT demonstrates even stronger gains, with its Structured Image Description performance reaching 88.75% in binary classification, a 3.76 percentage point improvement over its text-only counterpart. BERT-base follows a similar pattern, achieving 89.21% with Structured Image Description versus 85.09% with text alone.

Across all models, certain patterns emerge in prompting strategy effectiveness:

- Structured Image Description consistently outperforms other techniques, suggesting that well-organized, natural language descriptions are most effective for transformer models
- Simple Image Description and List of Objects show strong performance despite their simplicity, often achieving within 1-2 percentage points of the best results
- Scene Graph Analysis performs particularly well with larger models (87.91% with RoBERTa on 6-way classification) but shows diminished returns with smaller architectures
- Relational Mapping and Inconsistency Detection, while sophisticated, generally underperform simpler techniques, possibly due to the challenge of effectively encoding complex spatial and visual relationships in text

The performance gap between different prompting strategies widens with task complexity, becoming most pronounced in 6-way classification. For instance, RoBERTa-large shows a 20.51 percentage point spread between its best (87.95%) and worst (67.44%) prompting strategies in 6-way classification, compared to only 4.72 points in binary classification. This suggests that sophisticated prompting becomes increasingly crucial as the classification task grows more complex.

DeBERTa-v3-large demonstrates superior performance across all prompting techniques (Table 7), with the Structured Image Description strategy achieving the highest accuracy of 92.52%. Notable performance gains are also observed with Simple Image Description (92.06%) and Scene Graph Analysis (92.15%), suggesting that DeBERTa effectively leverages complex visual information when presented in textual form. The model shows significant improvement over its text-only baseline (87.64%), with an increase of 4.88 percentage points using Structured Image Description. Even the simplest approach, List of Objects, yields a modest improvement to 88.08%, while more sophisticated techniques like Relational Mapping achieve 90.72%. Interestingly, Inconsistency Detection shows minimal gains (87.85%), possibly due to the complexity of translating visual inconsistencies into text that the model can effectively process.

D Training Costs

The training costs for various language models were estimated based on Google Colab pricing of \$10 per 100 Compute Units (CUs). Table 8 provides a detailed breakdown of the training times and associated costs.

These cost estimates provide insights into the computational resources required for training different language models, highlighting the variations in training complexity and duration.

E Selection of Gemini 1.5 Pro for Vision-to-Text Translation

Our evaluation of various Vision-Language Models (VLMs) led to the selection of Gemini 1.5 Pro as the primary model for vision-to-text translation. This choice was driven by several key factors:

E.1 Technical Advantages

- **Context Window:** With a 2-million token context window, Gemini 1.5 Pro can handle images of varying complexity and generate detailed descriptions without truncation
- **Response Quality:** Produces more consistent and detailed outputs compared to open-source alternatives
- **Flexibility:** Supports multiple prompting strategies without triggering content restrictions

E.2 Limitations of Alternatives

E.2.1 Llama 3.2 Vision

- Built-in guardrails in the `mlx-community/Llama-3.2-11B-Vision-Instruct-8bit` model frequently block outputs for our prompting tasks
- Lower performance in zero-shot classification (63.92% vs. base accuracy)
- More restrictive in handling complex prompting strategies

E.2.2 GPT-4o

- Limited to 128K token context window
- Significantly higher operational costs
- Less suitable for large-scale deployment

E.3 Accessibility Considerations

- \$300 free trial credit enables initial deployment without significant investment
- Cost-effective for both research and small-scale applications
- Lower per-token costs compared to GPT-4o

The combination of superior technical capabilities, fewer restrictions, and better accessibility makes Gemini 1.5 Pro the optimal choice for our framework’s vision-to-text translation component. Its performance characteristics and cost structure align well with our goal of democratizing fake news detection capabilities.

F Prompting Techniques and Examples of Uni-Fakeddit-55k Dataset

This appendix provides detailed information about our six prompting techniques, including the exact prompts used and representative examples for each strategy.

Model	Prompting Technique	6-way	3-way	2-way
huawei-noah/ TinyBERT_General_4L_312D	Text Only	70.29%	82.84%	83.24%
	Text + List of Objects	77.02%	82.84%	85.05%
	Text + Simple Image Description	77.71%	85.28%	85.17%
	Text + Structured Image Description	80.08%	86.78%	87.36%
	Text + Relational Mapping	73.96%	81.23%	84.14%
	Text + Inconsistency Detection	75.74%	81.06%	81.89%
	Text + Scene Graph Analysis	74.91%	81.94%	85.05%
distilbert-base-uncased	Text Only	75.01%	84.83%	84.99%
	Text + List of Objects	82.09%	88.92%	88.50%
	Text + Simple Image Description	83.09%	87.24%	88.69%
	Text + Structured Image Description	83.98%	88.38%	88.75%
	Text + Relational Mapping	80.94%	86.28%	86.91%
	Text + Inconsistency Detection	80.55%	85.77%	85.66%
	Text + Scene Graph Analysis	83.86%	87.50%	87.64%
bert-base-uncased	Text Only	79.50%	84.09%	85.09%
	Text + List of Objects	83.10%	87.12%	87.45%
	Text + Simple Image Description	83.34%	88.16%	88.57%
	Text + Structured Image Description	85.25%	88.93%	89.21%
	Text + Relational Mapping	81.34%	86.48%	86.43%
	Text + Inconsistency Detection	80.95%	85.75%	85.95%
	Text + Scene Graph Analysis	85.24%	88.04%	88.35%
FacebookAI/roberta-large	Text Only	78.80%	86.99%	87.23%
	Text + List of Objects	86.60%	89.57%	89.92%
	Text + Simple Image Description	86.99%	90.77%	90.74%
	Text + Structured Image Description	87.95%	91.45%	91.88%
	Text + Relational Mapping	85.05%	89.41%	89.49%
	Text + Inconsistency Detection	67.44%	88.10%	89.01%
	Text + Scene Graph Analysis	87.91%	87.05%	87.16%

Table 6: Classification Performance Comparison (Accuracy) of BERT, DistilBERT, and RoBERTa on Uni-Fakeddit-55k

Model	Prompting Technique	Accuracy
microsoft/deberta-v3-large	Text Only	87.64%
	Text + List of Objects	88.08%
	Text + Simple Image Description	92.06%
	Text + Structured Image Description	92.52%
	Text + Relational Mapping	90.72%
	Text + Inconsistency Detection	87.85%
	Text + Scene Graph Analysis	92.15%

Table 7: Binary Classification Accuracy of DeBERTa on Uni-Fakeddit-55k

Model	Training Time	Cost
BERT	35 minutes	\$0.32
DistilBERT	22 minutes	\$0.282
TinyBERT	11 minutes	\$0.1465
RoBERTa	105 minutes	\$1.48
DeBERTa	135 minutes	\$1.91

Table 8: Language Model Training Costs on Google Colab

F.1 List of Objects Strategy

F.1.1 Prompt Template

Analyze the image and list all clearly visible objects and elements. Return a comma-separated list of distinct, identifiable objects. Focus on physical objects, not interpretations or actions. Be specific but concise in naming objects.

F.1.2 Example Outputs

This strategy focuses on creating an objective inventory of visible objects without interpretation or context. The comma-separated format ensures consistent parsing and processing in downstream tasks. Figures 5a and 5b present two sample inputs and the respective model outputs for this prompting strategy.

F.2 Simple Image Description Strategy

F.2.1 Prompt Template

Describe this image in exactly two sentences. Return only the description, with no additional text or explanation.

F.2.2 Example Outputs

This strategy focuses on generating concise, factual descriptions of image content. The two-sentence constraint ensures consistent length while allowing for both primary subject description and contextual details. Two sample inputs and their corresponding model outputs for this prompting strategy are illustrated in Figures 6a and 6b.

F.3 Structured Image Description Strategy

F.3.1 Prompt Template

Provide exactly two sentences about this image: First sentence: State only the observable facts - who and what is in the image, and where it takes place. Focus solely on what can be directly seen. Second sentence: Interpret the context -

explain the likely purpose, situation, or story behind what’s shown, including any relevant how or why elements. Return only these two sentences, with no additional text.

F.3.2 Example Outputs

This strategy employs a two-part structure to separate objective observations from contextual interpretation. The first sentence focuses on directly observable elements, while the second sentence provides deeper context and interpretation, enabling a more comprehensive understanding of the image content. The model outputs for two example inputs using this prompting strategy are depicted in Figures 7a and 7b.

F.4 Relational Mapping Strategy

F.4.1 Prompt Template

Analyze the spatial and interactive relationships between objects in this image. Return a JSON response with the following structure:

```
{
  "objects": [
    {
      "id": "unique_number",
      "name": "object_name",
      "location": "general_location_in_image"
    }
  ],
  "relationships": [
    {
      "subject_id": "id_of_first_object",
      "relation": "type_of_relationship",
      "object_id": "id_of_second_object",
      "confidence": "float_between_0_and_1"
    }
  ]
}
```

Include ONLY clearly visible relationships. For each relationship, assign a confidence score.

F.4.2 Example Outputs

This strategy generates structured representations of spatial and interactive relationships between objects in the image. The JSON format enables precise encoding of object locations and

their relationships, with confidence scores indicating the certainty of each relationship identification. Figures 8a and 9a showcase the model’s responses to two representative inputs when employing this prompting approach.

F.5 Inconsistency Detection Strategy

F.5.1 Prompt Template

Analyze this image for potential manipulation indicators or inconsistencies. Return a JSON response structured as follows:

```
{
  "lighting_analysis": {
    "inconsistencies": [
      {
        "description": "Detailed
          description of the lighting
          inconsistency",
        "location": "Where in the image
          this occurs",
        "confidence": float between 0-1,
        "affected_objects": ["list", "of",
          ", "affected", "objects"]
      }
    ],
    "overall_lighting_coherence":
      float between 0-1
  },
  "perspective_analysis": {
    "inconsistencies": [
      {
        "description": "Description of
          perspective or geometric
          anomaly",
        "location": "Where in the image
          this occurs",
        "confidence": float between 0-1,
        "affected_objects": ["list", "of",
          ", "affected", "objects"]
      }
    ],
    "overall_perspective_coherence":
      float between 0-1
  },
  "boundary_analysis": {
    "suspicious_edges": [
      {
        "object": "Name of object",
        "description": "Description of
          boundary anomaly",
        "location": "Where in the image
          this occurs",
```

```
"confidence": float between 0-1
    }
  ]
},
"overall_edge_quality": float
  between 0-1
},
"resolution_analysis": {
  "inconsistencies": [{
    "object": "Name of object",
    "description": "Description of
      resolution mismatch",
    "relative_to": "What it's
      inconsistent with",
    "confidence": float between 0-1
  }],
  "overall_resolution_coherence":
    float between 0-1
},
"metadata_analysis": {
  "jpeg_artifacts": boolean,
  "compression_inconsistencies":
    boolean,
  "noise_patterns": ["list", "of",
    "suspicious", "patterns"]
},
"summary": {
  "manipulation_likelihood": float
    between 0-1,
  "most_suspicious_elements": ["list", "of", "concerning", "elements"],
  "overall_assessment": "Brief
    summary of findings"}
}
```

Focus on identifying concrete, observable inconsistencies rather than speculation. Provide specific locations and descriptions for each identified anomaly.

F.5.2 Example Outputs

This strategy performs a comprehensive analysis of potential image manipulations by examining multiple technical aspects including lighting, perspective, boundaries, resolution, and metadata. The structured JSON output provides detailed assessments of each aspect with confidence scores and specific locations of any detected anomalies. Figures 10a and 11a show two examples of inputs and outputs using this prompting strategy.

F.6 Scene Graph Analysis Strategy

F.6.1 Prompt Template

Analyze this image to create a detailed scene graph with metadata. Return a JSON response structured as follows:

```
{
  "primary_subject": {
    "description": "Detailed
      description of the main
      subject/focus",
    "confidence": float between 0-1,
    "typical_context": boolean,
    "context_notes": "Explanation of
      context typicality"
  },
  "scene_elements": [
    {
      "object": "Name of the object or
        element",
      "location": "Location in the
        image",
      "confidence": float between 0-1,
      "relationships": [
        {
          "related_to": "Name of the
            related object",
          "relationship_type": "Type of
            relationship",
          "confidence": float between 0-1,
          "description": "Brief
            description of relationship"
        }
      ],
      "inconsistencies": [
        {
          "type": "Type of inconsistency",
          "description": "Description of
            visual inconsistency",
          "severity": float between 0-1
        }
      ]
    },
    {
      "metadata_analysis": {
        "image_quality": float between
          0-1,
        "quality_factors": {
          "resolution": float between 0-1,
          "clarity": float between 0-1,
          "lighting": float between 0-1
        },
        "potential_manipulations":
          [...],
        "technical_artifacts": [...]
```

```
},
  "analysis_summary": {
    "scene_complexity": float
      between 0-1,
    "manipulation_likelihood": float
      between 0-1,
    "overall_consistency": float
      between 0-1,
    "key_observations": ["list", "of
      ", "findings"]
  }
}
```

Focus on creating accurate relationships between elements and identifying any unusual or inconsistent aspects of the scene.

F.6.2 Example Outputs

This strategy creates comprehensive scene graphs that capture both the physical layout and the semantic relationships between objects in the image. The structured output includes confidence scores for detections, relationship descriptions, and detailed metadata analysis, enabling rich understanding of scene composition and potential inconsistencies. To demonstrate the effectiveness of this prompting strategy, Figures 12a and 13a display two sample inputs alongside their respective model-generated outputs.

G Training Hyperparameters

This appendix provides detailed information about the training configuration and hyperparameters used for each model in our experiments.

G.1 BERT Configuration

G.1.1 Model Architecture

- Base Model: bert-base-uncased
- Number of Labels: 6 (multi-class classification)
- Maximum Sequence Length: 128 tokens
- Model Size: 110M parameters

G.1.2 Training Parameters

- Batch Size: 8 (per device)
- Number of Epochs: 5
- Optimizer: AdamW
- Learning Rate: Default (5e-5)
- Weight Decay: 0.01
- Training/Validation Split: 70%/30%

G.1.3 Data Processing

- Text Input Format: [TEXT] + [OBJECTS] concatenation

- Tokenization: BERT tokenizer with truncation
- Padding Strategy: Max length (128 tokens)
- Random Seed: 42 (for reproducibility)

G.1.4 Training Strategy

- Evaluation Strategy: Per epoch
- Save Strategy: Per epoch
- Best Model Selection: Based on macro F1-score
- Early Stopping: Disabled
- Gradient Accumulation Steps: 1
- Mixed Precision Training: Enabled (FP16)

G.1.5 Evaluation Metrics

- Primary Metrics: Accuracy, Macro F1-score
- Secondary Metrics: Precision (macro and weighted)
- Per-class Metrics: Precision and F1-score
- Zero-division Handling: Set to 0 for undefined cases

G.1.6 Hardware Configuration

- Computing Platform: RTX 4060 Laptop GPU
- CUDA Version: 12.6
- Memory Utilization: 0.4GB VRAM (peak)
- Training Time: Approximately 1.16 hours

The training configuration was optimized for the specific characteristics of our dataset and hardware constraints. All experiments were conducted using the Hugging Face Transformers library (version 4.48.3) and PyTorch (version 2.6.0+cu126).

G.2 TinyBERT Configuration

G.2.1 Model Architecture

- Base Model: huawei-noah/TinyBERT_General_4L_312D
- Number of Labels: 6 (multi-class classification)
- Maximum Sequence Length: 512 tokens
- Model Size: 14.5M parameters
- Architecture: 4-layer, 312-dimensional compressed BERT

G.2.2 Training Parameters

- Batch Size: 16 (per device)
- Number of Epochs: 5
- Optimizer: AdamW
- Learning Rate: $2e-5$
- Weight Decay: 0.01
- Warmup Ratio: 0.1
- Training/Validation Split: 70%/30%

G.2.3 Data Processing

- Text Input Format: [TEXT] + [OBJECTS] concatenation
- Tokenization: TinyBERT tokenizer with truncation
- Padding Strategy: Max length (512 tokens)
- Random Seed: 42 (for reproducibility)

G.2.4 Training Strategy

- Evaluation Strategy: Every 1000 steps
- Save Strategy: Every 1000 steps
- Best Model Selection: Based on macro F1-score
- Early Stopping: Disabled
- Gradient Accumulation Steps: 2
- Mixed Precision Training: Enabled (FP16)
- Number of Data Loading Workers: 4

G.2.5 Evaluation Metrics

- Primary Metrics: Accuracy, Macro F1-score
- Secondary Metrics: Precision (macro and weighted)
- Per-class Metrics: Precision and F1-score
- Zero-division Handling: Set to 0 for undefined cases
- Evaluation Frequency: Every 1000 training steps

G.2.6 Hardware Configuration

- Computing Platform: RTX 4060 Laptop GPU
- CUDA Version: 12.6
- Memory Utilization: 0.2GB VRAM (peak)
- Training Time: Approximately 0.66 hours

Key differences from BERT include the use of a compressed 4-layer architecture, larger batch size (16 vs 8), more frequent evaluation (every 1000 steps vs per epoch), and higher learning rate ($2e-5$ vs $5e-5$). These modifications leverage TinyBERT's efficient architecture while maintaining competitive performance.

G.3 DistilBERT Configuration

G.3.1 Model Architecture

- Base Model: distilbert-base-uncased
- Number of Labels: 6 (multi-class classification)
- Maximum Sequence Length: 128 tokens
- Model Size: 66M parameters
- Architecture: Knowledge-distilled BERT with 6 layers

G.3.2 Training Parameters

- Batch Size: 8 (per device)
- Number of Epochs: 5
- Optimizer: AdamW
- Learning Rate: Default (5e-5)
- Weight Decay: 0.01
- Training/Validation Split: 70%/30%

G.3.3 Data Processing

- Text Input Format: [TEXT] + [OBJECTS] concatenation
- Tokenization: DistilBERT tokenizer with truncation
- Padding Strategy: Max length (128 tokens)
- Random Seed: 42 (for reproducibility)

G.3.4 Training Strategy

- Evaluation Strategy: Every 2000 steps
- Save Strategy: Every 2000 steps
- Best Model Selection: Based on macro F1-score
- Early Stopping: Disabled
- Gradient Accumulation Steps: 1
- Mixed Precision Training: Not enabled

G.3.5 Evaluation Metrics

- Primary Metrics: Accuracy, Macro F1-score
- Secondary Metrics: Precision (macro and weighted)
- Per-class Metrics: Precision and F1-score
- Zero-division Handling: Set to 0 for undefined cases
- Evaluation Frequency: Every 2000 training steps

G.3.6 Hardware Configuration

- Computing Platform: RTX 4060 Laptop GPU
- CUDA Version: 12.6
- Memory Utilization: 0.4GB VRAM (peak)
- Training Time: Approximately 1.5 hours

DistilBERT represents a middle ground between BERT and TinyBERT, using knowledge distillation to achieve a 40% size reduction from BERT while maintaining relatively strong performance. The configuration balances efficiency with model capacity, using similar batch sizes to BERT but with more frequent evaluation steps.

G.4 RoBERTa Configuration

G.4.1 Model Architecture

- Base Model: FacebookAI/roberta-large

- Number of Labels: 6 (multi-class classification)
- Maximum Sequence Length: 512 tokens
- Model Size: 355M parameters
- Architecture: 24-layer optimized BERT variant

G.4.2 Training Parameters

- Batch Size: 4 (per device)
- Effective Batch Size: 16 (with gradient accumulation)
- Number of Epochs: 5
- Optimizer: AdamW
- Learning Rate: 1e-5
- Weight Decay: 0.01
- Warmup Ratio: 0.1
- Training/Validation Split: 70%/30%

G.4.3 Data Processing

- Text Input Format: [TEXT] + [OBJECTS] concatenation
- Tokenization: RoBERTa tokenizer with truncation
- Padding Strategy: Max length (512 tokens)
- Random Seed: 42 (for reproducibility)

G.4.4 Training Strategy

- Evaluation Strategy: Every 2000 steps
- Save Strategy: Every 2000 steps
- Best Model Selection: Based on macro F1-score
- Early Stopping: Disabled
- Gradient Accumulation Steps: 4
- Mixed Precision Training: Enabled (FP16)
- Gradient Checkpointing: Enabled
- Number of Data Loading Workers: 4

G.4.5 Evaluation Metrics

- Primary Metrics: Accuracy, Macro F1-score
- Secondary Metrics: Precision (macro and weighted)
- Per-class Metrics: Precision and F1-score
- Zero-division Handling: Set to 0 for undefined cases
- Evaluation Frequency: Every 2000 training steps

G.4.6 Hardware Configuration

- Computing Platform: Nvidia A100
- CUDA Version: 12.4
- Memory Utilization: 7.2GB VRAM (peak)
- Training Time: Approximately 1.75 hours

RoBERTa-large is one of the two large models we used for the tests, requiring specific optimizations for training on limited hardware. These include reduced batch size, gradient accumulation, gradient checkpointing, and mixed precision training. Despite the computational demands, these optimizations enable effective training while maintaining the model's superior performance characteristics.

G.5 DeBERTa Configuration

G.5.1 Model Architecture

- Base Model: microsoft/deberta-v3-large
- Number of Labels: 6 (multi-class classification)
- Maximum Sequence Length: 512 tokens
- Model Size: 400M parameters
- Architecture: Enhanced BERT with disentangled attention

G.5.2 Training Parameters

- Batch Size: 4 (per device)
- Effective Batch Size: 16 (with gradient accumulation)
- Number of Epochs: 3
- Optimizer: AdamW
- Learning Rate: 1e-5
- Weight Decay: 0.01
- Warmup Ratio: 0.1
- Training/Validation Split: 70%/30%

G.5.3 Data Processing

- Text Input Format: [TEXT] + [OBJECTS] concatenation
- Tokenization: DeBERTa tokenizer with truncation
- Padding Strategy: Max length (512 tokens)
- Random Seed: 42 (for reproducibility)

G.5.4 Training Strategy

- Evaluation Strategy: Every 2000 steps
- Save Strategy: Every 2000 steps
- Best Model Selection: Based on macro F1-score
- Early Stopping: Disabled
- Gradient Accumulation Steps: 4
- Mixed Precision Training: Enabled (FP16)
- Gradient Checkpointing: Enabled
- Number of Data Loading Workers: 4

G.5.5 Evaluation Metrics

- Primary Metrics: Accuracy, Macro F1-score
- Secondary Metrics: Precision (macro and weighted)
- Per-class Metrics: Precision and F1-score
- Zero-division Handling: Set to 0 for undefined cases
- Evaluation Frequency: Every 2000 training steps

G.5.6 Hardware Configuration

- Computing Platform: Nvidia A100
- CUDA Version: 12.4
- Memory Utilization: 8.7GB VRAM
- Training Time: Approximately 2 hours

As our most advanced model, DeBERTa-v3-large incorporates disentangled attention mechanisms and enhanced mask decoder training, requiring similar memory optimizations to RoBERTa but with shorter training time due to faster convergence. The architecture's sophisticated attention mechanism enables better handling of complex textual relationships while maintaining computational efficiency through gradient checkpointing and mixed precision training.

Initial runs with 5 epochs resulted in overfitting. Subsequently, we switched to 3 epoch runs, which helped cut training time while deliver higher performance. Evaluation strategy is set to 2,000 steps to further reduce computational cost.

G.6 Evaluation Methodology

Our evaluation framework combines both periodic monitoring during training and comprehensive final assessment. During training, we implement regular evaluation checkpoints to track model progress and ensure stable optimization:

G.6.1 Training-time Evaluation

Models are evaluated on the test set at regular intervals during training:

- TinyBERT: Every 1000 steps
- BERT and DistilBERT: Every 2000 steps
- RoBERTa and DeBERTa: Every 2000 steps with gradient accumulation

These intermediate evaluations help monitor:

- Convergence patterns
- Potential overfitting
- Learning rate effectiveness
- Model stability

G.6.2 Final Evaluation

The final evaluation is conducted after completing the full training regime:

- BERT, DistilBERT, TinyBERT, and RoBERTa: 5 complete epochs
- DeBERTa: 3 complete epochs (faster convergence observed)

For each model, we compute:

- Overall accuracy
- Macro and weighted precision
- Macro and weighted F1-scores
- Per-class precision and F1-scores

The evaluation metrics are calculated on the held-out test set (30% of the dataset) using scikit-learn’s implementation of precision, F1-score, and accuracy metrics. All models use identical train-test splits (stratified by class) to ensure fair comparison, with results reported as percentages for clarity.

H Vision-Language Model Testing Configuration

This appendix details the setup and configuration used for zero-shot testing with Vision-Language Models (VLMs).

H.1 Llama 3.2 Vision Testing Setup

H.1.1 Model Configuration

- Base Model: unsloth/Llama-3.2-11B-Vision-Instruct
- Model Size: 11B parameters
- Quantization: 4-bit quantization with NF4 format
- Double Quantization: Enabled
- Dtype: BFloat16
- Device Mapping: Automatic

H.1.2 Prompt Template

```
Analyze this image and its title: "{
  title}"
```

```
Is this a fake news post or a real news
post?
```

```
Respond with either FAKE or REAL,
followed by your explanation.
```

```
Title: {title}
```

H.1.3 Processing Configuration

- Maximum Generated Tokens: 100
- Image Format: RGB (converted if necessary)
- Batch Size: 1 (sequential processing)
- Memory Optimization: 4-bit quantization

H.1.4 Evaluation Setup

- Dataset Size: 55,000 samples
- Output Processing: First word extraction (FAKE/REAL)
- Label Mapping: FAKE \rightarrow 0, REAL \rightarrow 1
- Default Fallback: FAKE (conservative approach)
- Progress Monitoring: Accuracy reported every 100 samples

H.1.5 Hardware Requirements

- GPU: NVIDIA RTX 4090
- VRAM Usage: 12GB (with quantization)
- Storage: 50GB for model and dataset
- Processing Time: Approximately 6 hours for full dataset

Results from this configuration achieved 63.92% accuracy on binary classification, demonstrating the model’s zero-shot capabilities in fake news detection without any fine-tuning.

H.2 Video LLaVA Testing Setup

H.2.1 Model Configuration

- Base Model: LanguageBind/Video-LLaVA-7B-hf
- Model Size: 7B parameters
- Model Type: Conditional Generation
- Quantization: None (full precision)
- Device Mapping: Single GPU

H.2.2 Prompt Template

```
USER: <image> Given this image and its
title: '{title}',
is this a fake news post or a real news
post?
```

```
Respond with either FAKE or REAL,
followed by your explanation.
```

```
ASSISTANT:
```

H.2.3 Processing Configuration

- Maximum Generated Tokens: 100
- Image Format: RGB (converted if necessary)
- Batch Size: 1 (sequential processing)
- Padding: Enabled
- Special Token Handling: Customized EOS and PAD tokens

H.2.4 Evaluation Setup

- Dataset Size: 10,000 samples
- Output Processing: First word extraction (FAKE/REAL)
- Label Mapping: FAKE \rightarrow 0, REAL \rightarrow 1
- Default Fallback: FAKE (conservative approach)
- Progress Monitoring: Accuracy reported every 100 samples

H.2.5 Hardware Requirements

- GPU: NVIDIA RTX 4090
- VRAM Usage: 16GB
- Storage: 30GB for model and dataset
- Processing Time: Approximately 2 hours for 10k samples

Results from this configuration achieved 59.34% accuracy on binary classification. Despite being designed for video understanding, the model demonstrated moderate capability in static image analysis for fake news detection.

H.3 InstructBLIP Testing Setup

H.3.1 Model Configuration

- Base Model: Salesforce/instructblip-vicuna-7b
- Model Size: 7B parameters
- Model Type: Conditional Generation with BLIP architecture
- Quantization: 4-bit quantization with NF4 format
- Double Quantization: Enabled
- Dtype: BFloat16
- Device Mapping: Automatic

H.3.2 Prompt Template

```
Analyze this image and its title: "{
  title}"
```

Is this a fake news post or a real news post?

Respond with either FAKE or REAL, followed by your explanation.

H.3.3 Generation Parameters

- Maximum Length: 256 tokens
- Minimum Length: 1 token
- Number of Beams: 5
- Top-p: 0.9
- Repetition Penalty: 1.5

- Length Penalty: 1.0
- Temperature: 1.0
- Sampling: Disabled

H.3.4 Processing Configuration

- Image Format: RGB (converted if necessary)
- Batch Size: 1 (sequential processing)
- Memory Optimization: 4-bit quantization
- Special Token Handling: Skip special tokens in decoding

H.3.5 Evaluation Setup

- Dataset Size: 55,000 samples
- Output Processing: First word extraction (FAKE/REAL)
- Label Mapping: FAKE \rightarrow 0, REAL \rightarrow 1
- Default Fallback: FAKE (conservative approach)
- Progress Monitoring: Accuracy reported every 100 samples

H.3.6 Hardware Requirements

- GPU: NVIDIA RTX 4090
- VRAM Usage: 10GB (with quantization)
- Storage: 25GB for model and dataset
- Processing Time: Approximately 5 hours for full dataset

Results from this configuration achieved 59.35% accuracy on binary classification. The model demonstrates performance comparable to Video-LLaVA despite their architectural differences, suggesting similar capabilities in fake news detection tasks.



Input Image 1: Police incident scene

Caption: Use of deadly force by police disappears on Richmond streets

Model Output: Car exhaust pipe, Car bumper, Car body, Gun shadow, Hand shadow, Reflection of a person, Reflection of a vehicle, Reflection of trees/objects, Road reflection



Input Image 1: UN press conference

Caption: U.S., Britain, France, others skip nuclear weapons ban treaty talks

Model Output: Nikki Haley, then-U.S. Ambassador to the United Nations, speaks at a podium, surrounded by other officials. They appear to be at a press conference or similar official event.



Input Image 2: Theme park concept art

Caption: Viacom's proposed Nickelodeon-themed floating resort to be situated at Coron Palawan

Model Output: Roller coaster, roller coaster track, glove-shaped entrance, sign reading "Glove World", glove-shaped Ferris wheel, glove-shaped ride, fence, glove-shaped topiary, light post with flag, SpongeBob SquarePants, Patrick Star, road/sidewalk, jellyfish, glove decorations, red and white striped tent/awning



Input Image 2: Teapot modification

Caption: Use plastic tubing to make a more accurate teapot spout

Model Output: A small, white teapot sits on a brown table. The teapot's lid is slightly askew, revealing a stained interior, and the spout has a piece of clear tape affixed to it.



Input Image 1: Walt Disney at Disneyland

Caption: Walt Disney, deep in thought, after everyone's left the park

Model Output: Walt Disney sits on a green bench, facing a large Victorian-style building with a clock tower, situated in a paved plaza with trees. This photo likely captures Disney observing his newly opened Disneyland, perhaps reflecting on its creation or planning future additions and improvements.



Input Image 1: Pet portrait

Caption: Chihuahua in a hat

Model Output:

```
{
  "objects": [
    {"id": "1", "name": "chihuahua", "location": "center"},
    {"id": "2", "name": "sweater", "location": "center"},
    {"id": "3", "name": "chair", "location": "everywhere"},
    {"id": "4", "name": "cushion", "location": "underneath dog"},
    {"id": "5", "name": "blanket/pillow", "location": "right side"},
    {"id": "6", "name": "shelf/table edge", "location": "left side"},
    {"id": "7", "name": "red and white object", "location": "top left corner"}
  ],
  "relationships": [
    {"subject_id": "1", "relation": "wearing", "object_id": "2", "confidence": 1.0},
    {"subject_id": "1", "relation": "lying on", "object_id": "3", "confidence": 1.0},
    {"subject_id": "1", "relation": "lying on", "object_id": "4", "confidence": 1.0},
    {"subject_id": "3", "relation": "next to", "object_id": "5", "confidence": 1.0},
    {"subject_id": "3", "relation": "partially occluding", "object_id": "6", "confidence": 0.9},
    {"subject_id": "6", "relation": "supporting", "object_id": "7", "confidence": 0.8}
  ]
}
```



Input Image 2: Octopus underwater

Caption: This octopus discovered a coconut on the bottom of the ocean you won't believe what happened next

Model Output: An octopus, partially camouflaged against a rocky, green seabed, holds a large crab in its tentacles underwater. The octopus is likely hunting and has captured the crab as prey, using its tentacles to restrain it before consuming it.



Input Image 2: Fire aftermath

Caption: Inspectors tried to access Oakland warehouse before deadly fire

Model Output:

```
{
  "objects": [
    {
      "id": 1,
      "name": "burned building",
      "location": "center"
    },
    {
      "id": 2,
      "name": "debris pile",
      "location": "bottom center"
    },
    {
      "id": 3,
      "name": "truck",
      "location": "bottom left"
    },
    {
      "id": 4,
      "name": "firefighters",
      "location": "center"
    },
    {
      "id": 5,
      "name": "construction equipment",
      "location": "bottom right"
    },
    {
      "id": 6,
      "name": "white tent",
      "location": "bottom center"
    },
    {
      "id": 7,
      "name": "adjacent building",
      "location": "right"
    }
  ],
  "relationships": [
    {
      "subject_id": 2,
      "relation": "in front of",
      "object_id": 1,
      "confidence": 1.0
    },
    {
      "subject_id": 3,
      "relation": "next to",
      "object_id": 2,
      "confidence": 0.9
    },
    {
      "subject_id": 4,
      "relation": "inspecting",
      "object_id": 1,
      "confidence": 0.8
    },
    {
      "subject_id": 4,
      "relation": "near",
      "object_id": 2,
      "confidence": 0.7
    },
    {
      "subject_id": 5,
      "relation": "parked near",
      "object_id": 1,
      "confidence": 0.9
    },
    {
      "subject_id": 6,
      "relation": "in front of",
      "object_id": 1,
      "confidence": 0.8
    },
    {
      "subject_id": 7,
      "relation": "attached to",
      "object_id": 1,
      "confidence": 0.9
    }
  ]
}
```



Input Image 1: Artistic rendering

Caption: Flooded boiler room in Washington a few filters over a dog

Model Output:

```
{
  "lighting_analysis": {
    "inconsistencies": [],
    "overall_lighting_coherence": 0.9
  },
  "perspective_analysis": {
    "inconsistencies": [
      {
        "description": "The figure's limbs and body seem to defy normal anatomical proportions and perspective, appearing stretched and distorted.",
        "location": "Throughout the figure",
        "confidence": 0.8,
        "affected_objects": ["Figure"]
      }
    ],
    "overall_perspective_coherence": 0.5
  },
  "boundary_analysis": {
    "suspicious_edges": [],
    "overall_edge_quality": 0.9
  },
  "resolution_analysis": {
    "inconsistencies": [],
    "overall_resolution_coherence": 0.9
  },
  "metadata_analysis": {
    "jpeg_artifacts": false,
    "compression_inconsistencies": false,
    "noise_patterns": []
  },
  "summary": {
    "manipulation_likelihood": 0.1,
    "most_suspicious_elements": [],
    "overall_assessment": "The image is likely an artistic creation with stylized, non-realistic proportions. No clear signs of image manipulation were detected. The distorted anatomy is consistent with artistic expression rather than technical manipulation."
  }
}
```



Input Image 2: Restaurant review

Caption: Uptown Reviews - Waterboarding at Guantanamo Bay

Model Output:

```
{
  "lighting_analysis": {
    "inconsistencies": [],
    "overall_lighting_coherence": 0.95,
    "perspective_analysis": {
      "inconsistencies": [],
      "overall_perspective_coherence": 0.95,
      "boundary_analysis": {
        "suspicious_edges": [],
        "overall_edge_quality": 0.95,
        "resolution_analysis": {
          "inconsistencies": [],
          "overall_resolution_coherence": 0.95,
          "metadata_analysis": {
            "jpeg_artifacts": false,
            "compression_inconsistencies": false,
            "noise_patterns": [],
            "summary": {
              "manipulation_likelihood": 0.05,
              "most_suspicious_elements": [],
              "overall_assessment": "No obvious signs of image manipulation were detected. The lighting, perspective, boundaries, and resolution appear consistent throughout the image. There are no discernible compression artifacts or unusual noise patterns."
            }
          }
        }
      }
    }
  }
}
```



Input Image 1: Wildlife photograph

Caption: Iguana eating a flower

Model Output:

```
{
  "primary_subject": {
    "description": "A green iguana is consuming a red, spiky flower.",
    "confidence": 0.95,
    "typical_context": true,
    "context_notes": "Iguanas are known to eat flowers and vegetation, so this behavior is within their natural diet.",
    "scene_elements": [
      {
        "object": "Iguana",
        "location": "Center",
        "confidence": 0.99,
        "relationships": [
          {
            "related_to": "Flower",
            "relationship_type": "Eating",
            "confidence": 0.95,
            "description": "The iguana's mouth is open and around the flower, indicating it is consuming it."
          },
          {
            "related_to": "Leaves",
            "relationship_type": "Near",
            "confidence": 0.90,
            "description": "The iguana is surrounded by green leaves, suggesting a natural habitat or enclosure."
          }
        ]
      },
      {
        "object": "Flower",
        "location": "Left-center",
        "confidence": 0.90,
        "relationships": [
          {
            "related_to": "Iguana",
            "relationship_type": "Being eaten by",
            "confidence": 0.95,
            "description": "The flower is in the iguana's mouth."
          }
        ]
      },
      {
        "object": "Leaves",
        "location": "Background",
        "confidence": 0.95,
        "relationships": [
          {
            "related_to": "Iguana",
            "relationship_type": "Surrounding",
            "confidence": 0.90,
            "description": "The leaves form the background and immediate environment of the iguana."
          }
        ]
      }
    ],
    "inconsistencies": [],
    "metadata_analysis": {
      "image_quality": 0.85,
      "quality_factors": {
        "resolution": 0.80,
        "clarity": 0.90,
        "lighting": 0.80,
        "potential_manipulations": [],
        "technical_artifacts": [
          {
            "type": "Slight noise",
            "location": "Darker areas of the leaves",
            "severity": 0.1
          }
        ],
        "analysis_summary": {
          "scene_complexity": 0.5,
          "manipulation_likelihood": 0.05,
          "overall_consistency": 0.95
        }
      }
    }
  }
}
```

```
"key_observations":["The image depicts a natural interaction between an iguana and a flower in a leafy environment.", "The image quality is good with slight noise in darker areas .", "No obvious signs of manipulation were detected."]]}
```



Input Image 2: Yard decoration

Caption: The name of this shop is almost Harry Potter

Model Output:

```
{ "primary_subject": { "description": "A yard decorated with concrete statues and figures .", "confidence": 0.9, "typical_context": false, "context_notes": "While yards can have decorations, the sheer number and apparent focus on concrete statues makes this context less typical than a yard with a few gnomes or other common decorations." }, "scene_elements": [ { "object": "Concrete statues", "location": "Center, foreground", "confidence": 0.95, "relationships": [ { "related_to": "Yard", "relationship_type": "Located in", "confidence": 1.0, "description": "The statues are placed throughout the yard ."}, { "related_to": "Fence", "relationship_type": "Enclosed by", "confidence": 0.8, "description": "A chain-link fence appears to enclose the area where the statues are displayed." } ] }, { "object": "Yard", "location": "Foreground", "confidence": 1.0,
```

```
"inconsistencies": [] }, { "object": "Cars", "location": "Left, middleground", "confidence": 0.9, "relationships": [], "inconsistencies": [] }, { "object": "Trees", "location": "Background and throughout the scene", "confidence": 0.95, "relationships": [], "inconsistencies": [] }, { "object": "Sign", "location": "Center-left, above the statues", "confidence": 0.8, "relationships": [ { "related_to": "Concrete statues", "relationship_type": "Relates to", "confidence": 0.7, "description": "Likely a sign advertising the sale or creation of the statues." } ] }, { "object": "Fence", "location": "Surrounding the statues", "confidence": 0.8, "relationships": [ { "related_to": "Concrete Statues", "relationship_type": "Encloses", "confidence": 0.9, "description": "The fence likely serves to enclose the statue display area." } ] }, { "object": "Power lines", "location": "Across the image", "confidence": 0.9, "relationships": [], "inconsistencies": [] }, { "metadata_analysis": { "image_quality": 0.75, "quality_factors": { "resolution": 0.8, "clarity": 0.8, "lighting": 0.7 }, "potential_manipulations": [], "technical_artifacts": [] }, "analysis_summary": { "scene_complexity": 0.6, "manipulation_likelihood": 0.05, "overall_consistency": 0.95, "key_observations": [ "The primary subject is a collection of concrete statues in a yard. The scene is generally consistent and appears to be an unedited photo." ] } ] }
```